Chiang Mai J. Sci. 2008; 35(2) : 355-369
www.science.cmu.ac.th/journal-science/josci.html
Contributed Paper

The Underpotential Determination of Lead Using the Laboratory-made Gold Electrode Flow Cell

Prinya Masawat* [a] and Saisunee Liawruangrath [b]
[a] Department of Chemistry, Faculty of Science, Naresuan University, Phitsanulok, 65000, Thailand.
[b] Department of Chemistry, Faculty of Science, Chiang Mai University, Chiang Mai, 50200, Thailand.
*Author for correspondence; e-mail: prinyam@nu.ac.th

Received: 16 January 2008
Accepted: 21 February 2008.

ABSTRACT

The analysis of lead(II) by continuous flow square-wave anodic stripping voltammetry (SWASV) at a gold electrode flow cell is described. Various experimental variables have been optimized to yield low detection limit and good precision. The detection limits for a 30 s and 600 s electrodeposition were 3.5 and 0.38 $\mu g\ L^{-1}$, respectively. The recoveries were found to be 113 $\pm$ 1.8 % and 108 $\pm$ 2.3 % (n=5) in spiked drinking water samples and 110 $\pm$ 4.8 % and 106 $\pm$ 3.4% (n=5) in spiked tap water samples. Reproducibility on measurement of solution containing 5 $\mu g\ L^{-1}$ lead(II) (%R.S.D., n = 20) was 2.1 %. Measurements in the presence of typical interferences such as copper(II), cadmium(II), zinc(II), iron(II), chromium(VI), and mercury are also reported.

Keywords: flow cell, lead, gold electrode, square-wave anodic stripping voltammetry, flow injection analysis.

1. INTRODUCTION

The determination of trace levels of lead is a continuing research interest due to its toxicity and accumulation in the environment and living organisms [1]. Flow injection (FI) methods of separation and preconcentration have been utilised to enhance sensitivity and selectivity in the determinations of trace metals [2,3]. The methods have significant advantages over their batch counterparts, e.g. high sample throughput, enrichment efficiencies and reproducibility, low reagent and sample consumption, less risk of contamination and simple automated operation. A number of method for the determination of lead in biological and environmental samples are reported in the literature including on-line preconcentration followed by atomic absorption spectrophotometry [4-6], FI with ICP-MS detection [7,8], FI with spectrophotometric detection [9-11], and FI potentiometry by poly(vinyl chloride)-membrane electrode with substituted azacrown ionophores [12].

For analytes such as lead, electrochemical stripping analysis is considered to be a powerful technique with excellent detection limits, selectivity, and the possibility of

simultaneous multielement detection [13]. The combination of electrochemical stripping techniques with the advantages of flow injection for lead determination have been demonstrated by several workers [14-18]: Mannino [14] used potentiometric stripping analysis in a continuous flow system containing a thin-layer cell with two mercury film modified glassy carbon electrodes for simultaneous determination of lead and tin in fruit juice and soft drinks. Matysik and Werner [15] adapted a fused silica capillary system for flow injection using anodic stripping voltammetry at mercury-coated platinum microdisc electrodes for trace metal determination in tears. Jaenicke et al. [16] described an automated electrochemical method, using flow injection analysis with a wall-jet detector for determination of lead in blood. In this application, mercury film electrode (MFE) modified with a Nafion®-membrane coating was used. The MFE was also employed by Silva and Masini [17] for the determination of copper, lead, cadmium and zinc in river sediment extracts by sequential injection anodic stripping voltammetry. Mercury-free methods of analysis are highly desirable since future regulations and occupational health considerations may severely restrict the use of mercury as an electrode material. Staden and Matoetoe [18] simultaneously determined copper, lead, cadmium and zinc in water samples using differential pulse anodic stripping voltammetry in a flow system with a mercury-free glassy carbon electrode. The detection limit of lead was found to be 16.6 μg L^{-1} for 3 min deposition. Unfortunately, with a re-usable glassy carbon electrode, there are problems of contamination and sample carryover and in continuous use there must be concerns with drift and the need for recalibration.

In an earlier paper [19] we have demonstrated lead(II) detection using sputtered gold-coated screen-printed carbon electrode (SPCE) in a flow system. The method showed good detection limits (0.8 μg L^{-1} for 120 s deposition) and reproducibility (%R.S.D. = 2.9 %) but the low cost sensors were limited to use in a disposable format since a maximum of 5-7 determinations could be made with the same strip. In this paper we describe the use of gold disc mini electrodes in thin layer and wall jet flow cells suitable for a continuous measurement regime. Solid gold electrode [13] without any modifying offers a very favorable electron-transfer kinetics and a large anodic potential range. The lifetime of the solid gold electrode is much longer than the gold-coated SPCE. The long-term response stability of solid gold electrode was found for lead detection if using a pulse potential (cleaning/reactivation) cycle, which is common in flow amperometry, or via an appropriate chemical treatment.

2. EXPERIMENTAL

2.1 Chemicals and Reagents

All chemicals were of analytical-reagent grade and used as received. Deionized water was obtained from a Prima Reverse Osmosis, Maxima water purification system (Elga Ltd., UK). Reagents used were lead nitrate (99.0 %, AVOCADO, Research Chemicals Ltd, UK), acetic acid (100 %, BDH, UK), sodium acetate trihydrate (99.0 %, SIGMA®, UK), potassium chloride (99.5% BDH, UK), and nitric acid (69 %, BDH, UK). The copper, cadmium, zinc, iron, chromium, and mercury stock solutions (1000 ppm atomic absorption standards) were obtained from Fison Scientific Equipment, UK. The carrier solution was pH 4.5 acetate buffer (thin-layer cell) and 10 mM KCl in pH 4.5 acetate buffer (wall-jet cell). Stock solution of 1000 ppm Pb(II) was prepared by dissolving 0.16 g of $Pb(NO_3)_2$

in carrier solution and diluting to 100 mL. Working standards were prepared by dilution of the primary stock solution with the carrier solution. The drinking water samples were collected in Gordon House, School of Biological and Chemical Science, Birkbeck College, University of London and the tap water samples were collected in G18 Christopher Ingold Laboratories, University College London. Glassware and polythene containers were similarly soaked in 12 % nitric acid [20] for 48 hours, and then rinsed three times with deionized water and dried in air before use.

2.2 AppAratus

All voltammetric experiments were performed using a Metrohm Ion Analyzer Model 757 VA Computrace (Metrohm, Switzerland) and an Autolab PGSTAT20 (The Netherlands). Peristaltic pumps (Watson-Marlow, UK and Eyela MP3, Japan) were used for sample propulsion. All connecting tubing (0.5 mm i.d.) was supplied by Omnifit. A specially fabricated thin-layer cell containing the mini gold disc electrode and mini Ag/AgCl reference electrode, and a wall-jet cell incorporating with a gold disc electrode were used.

2.3 The Designed Flow Cells

The design of the thin-layer cell is shown in Figure 1. It consists of two Perspex blocks; (1) a reference block with both a socket for a Ag/AgCl (3M KCl) reference electrode (EA 442, Metrohm, Switzerland) and inlet and outlet for sample solution, and (2) a working block with a socket for a conventional solid gold electrode (5 mm in diameter, EA 286/3, Metrohm, Switzerland). An auxiliary electrode positioned between the two Perspex blocks was made from a plate of stainless steel (0.88 mm thickness, 5.4 cm x 2 cm rectangle) with a central electrode access hole (2 mm in diameter) and inlet and outlet holes (1 mm in diameter) in its body. The Polyester and/or Polypropylene spacer (0.05-0.50 mm thickness, Plastic Shim Pack, RS components, U.K.) with a central hole (1.9 cm x 0.2 cm quadrilateral) was positioned over the gold disc electrode before a plate of stainless steel auxiliary electrode and between the two Perspex blocks to seal the cell and form the flow chamber. The assembly was clamped together using an aluminum plate base. The volume of the thin-layer flow cell was estimated as 10 μL.

The comparative experiments were performed using a laboratory-made wall-jet cell that has been described elsewhere [21]. The working electrode was a gold disc (3 mm in diameter, Koch-Light Laboratories Ltd., UK). Before use, the surface of the gold disc working electrode housed in the Perspex working block was rinsed with distilled water followed by methanol to flush away any encrusted material on the surface, and gently wiped dry using a fresh lab tissue. Subsequently polishing was carried out manually on a polishing pad using the MF-2054 1-μm diamond polish slurry (Bioanalytical Systems, IN). After 1-2 min diamond polishing, the electrodes were rinsed with methanol followed by polishing with CF-1050 alumina slurry (Bioanalytical Systems, IN) for 1-2 min. The electrodes were then rinsed with distilled water and were sonicated for 5 min. The electrode was rinsed again with distilled water followed by small amount of methanol and wiped dry. The electrode now is ready to use.

2.4 Accumulation and Voltammetric Procedures

Cyclic voltammetry was performed to investigate the possible accumulation of Pb^{2+} at the gold disc electrode housed in the specially fabricated thin-layer flow cell. The oxygen-free solution of carrier solution and 100 mg

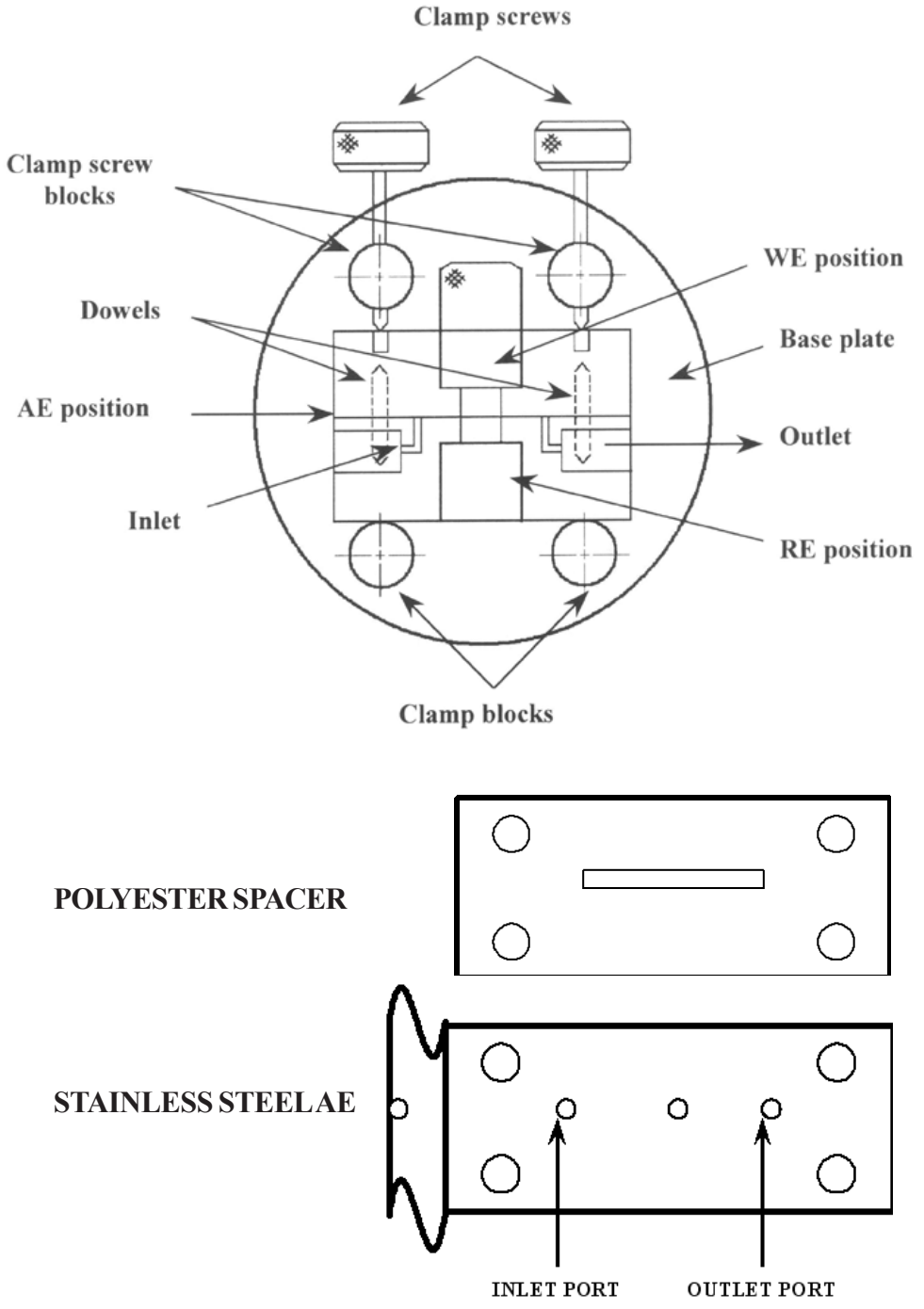

Figure 1. Schematic plan view of the thin-layer cell designed for incorporating with a gold disc electrode.

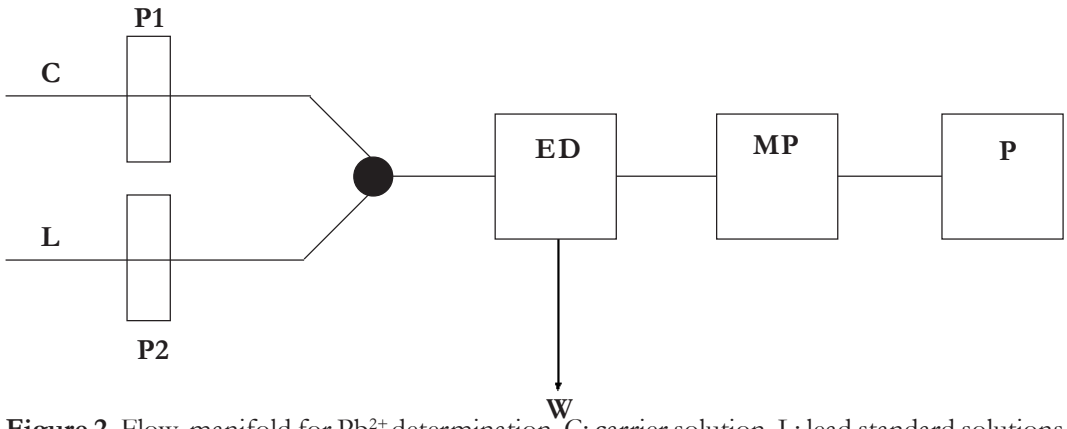

Figure 2. Flow manifold for Pb^{2+} determination. C: carrier solution, L: lead standard solutions in carrier solution, P1, P2: peristaltic pumps, ED: thin-layer or wall-jet flow cell with a gold disc electrode electrochemical detector, MP: Metrohm Potentiostat, P: Printer, W: waste. ● : three-port valve.

L^{-1} Pb^{2+} in carrier solution were pumped through the cell at the flow rate of 1 mL min^{-1} for 1 min to allow any accumulation to occur at open circuit, then the flowing solutions were stopped for 5 s. The voltage was subsequently scanned from 0 V to –1.0 V, then reverse to 0 V at the voltage step 6 mV. Scan rates were varied between 10 and 300 mV s^{-1}.

Quantitative determination of Pb^{2+} were performed using square-wave anodic stripping voltammetry. The procedure with the flow manifold illustrated in Figure 2 is described as follows:

1. For pre-conditioning of the electrode, the peristaltic pump, P1, was activated, pumping carrier solution through the flow cell, ED, at a rate of 1.0 mL min^{-1}. During the pre-conditioning a potential of +0.8 V vs Ag/AgCl reference electrode was applied to the gold disc working electrode for 50 s.
2. For underpotential deposition of Pb^{2+}, P1 was stopped and P2 was activated, pumping Pb^{2+} standard solution in carrier solution through the flow cell at a rate of 1.0 mL min^{-1}. Simultaneously, the potentiostat applies a potential of –0.7 V vs Ag/AgCl reference electrode to the gold disc working electrode for 30 s.
3. Following the electrodeposition and a 10 s rest period (with both pumps stopped), the square-wave anodic stripping voltammogram was recorded from –1.0 V using a voltage step of 5 mV, amplitude of 25 mV, frequency of 15 Hz, and sweep rate of 75.5 mV s^{-1}.
4. Before making repeated measurements the potential was held at +0.8 V for 50 s while P1 was activated to ensure complete removal of previous deposits. Background current associated with the residual dissolved oxygen and the gold surface reactions was subtracted from the square-wave voltammogram to provide a background compensation.

For evaluation of the method we determined Pb^{2+} in drinking and tap water using the method of standard addition. All data was obtained at room temperature.

3. RESULTS AND DISCUSSION

3.1 Accumulation and Cyclic Voltammetric Behavior of Pb^{2+} at the Gold Disc Electrode

The fundamental basis of the accumulation of Pb^{2+} on gold disc electrode is

underpotential deposition (UPD). UPD [22-24] is the electrochemical deposition of foreign metals onto substrates at potentials positive relative to the reversible Nernst potential for bulk deposition. The formation of a stable overlayer before the bulk deposition potential is possible because the adatom-substrate bond is thermodynamically more favorable to the adatom-adatom bond. For this reason, UPD is usually limited to a monolayer in extent, and the resulting structure of the UPD adlayer is strongly influenced by the substrate. Surface charge for the adsorbed UPD-Pb and bulk-Pb films (Q_c) on gold-coated SPCE was determined by simple integration of respective cyclic voltammograms using a built-in Autolab program. The equation of $Q = nFA\Gamma_s$ was used for the calculation of surface coverage (Γ_s) of the films, where n, F, and A represent number of electron transfer, Faraday constant, and electrode area, respectively.

The typical cyclic voltammogram of Pb^{2+} (100 mg L^{-1}) on the gold disc electrode under various scan rate are shown in Figure 3. At the scan of 10 mV s^{-1} (Figure 3a), the two anodic peaks at around –0.5 V (a1) and –0.3 V (a2) were observed. The surface charge (Q_c) was calculated to be 56.7 mC cm^{-2} corresponding to a Γ_s = 2.94 x 10^{-7} mol cm^{-2} specifying the multilayer formation of the bulk-Pb at this relatively slower scan rate. When the scan rate was increased to 100 mV s^{-1} (Figure 3b) the well-defined anodic peak at around –0.3 V was observed. In this case the surface charge was calculated to be 5.56 mC cm^{-2} corresponding to a Γ_s = 2.88 x 10^{-8} mol cm^{-2} specifying the small monolayer coverage of the UPD-Pb film. A complete diminishing of the bulk-Pb peak was noticed when the scan rate was further increased to 300 mV s^{-1} (Figure 3c). The variation of bulk-Pb and UPD-Pb with scan rate indicated different formation rates of these two processed.

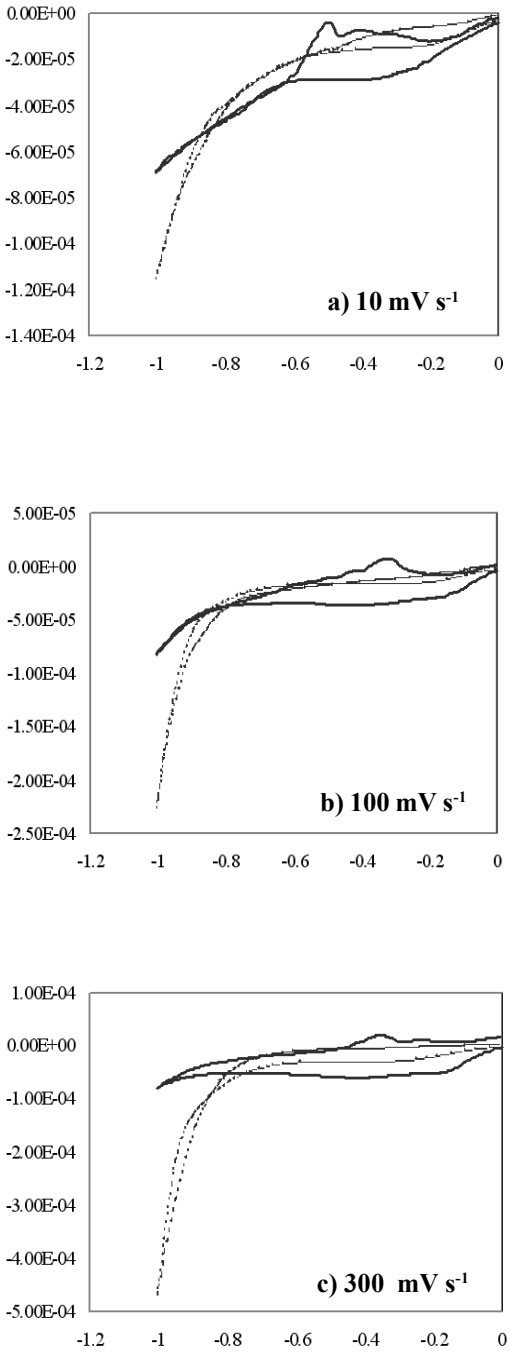

Figure 3. Cyclic voltammetry of the gold disc electrode with (solid lines) and without (broken lines) 100 mg L^{-1} Pb^{2+} in pH 4.5 acetate buffer at various scan rates of (a) 10, (b) 100, and (c) 300 mV s^{-1}.

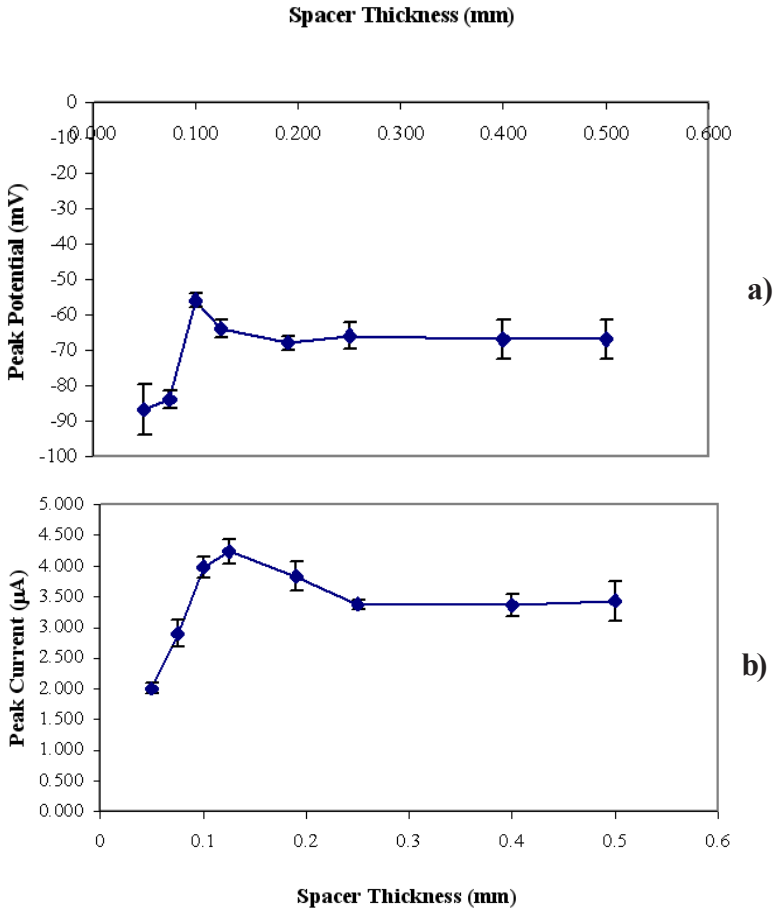

Figure 4. Dependence of the spacer thickness on (a) the peak potential and (b) on the peak stripping current for 50 μg L^{-1} Pb^{2+} in pH 4.5 acetate buffer at 1.0 mL min^{-1} flow rate. Square-wave anodic stripping voltammetry for Pb^{2+} at gold disc electrode, deposition potential ,–0.7 V vs Ag/AgCl; deposition time, 60 s; voltage step, 5 mV; amplitude, 25 mV; Frequency, 15 Hz; sweep rate, 75.5 mV s^{-1}. n = 3.

3.2 Anodic Stripping Analysis Using the Designed Thin-layer Cell

Square-wave voltammetry was used to follow the lead stripping process at the gold disc electrode because it offers certain advantages over the linear sweep and differential pulse voltammetry for rapid analysis [13]. The analysis time was drastically reduced; a complete voltammogram can be recorded within a few seconds, compared with about 2-3 min in differential pulse voltammetry.

Initial studies were performed to investigate the effect of spacer thickness on the square-wave anodic stripping voltammetric behavior of Pb^{2+} using gold disc electrode housed in the specially fabricated thin-layer cell (Figure 1). The spacer thickness of 0.050, 0.075, 0.100, 0.125, 0.190, 0.250 (Polyester), 0.400, and 0.500 (Polypropylene) mm were used. Figure 4 shows effect of spacer thickness on peak potential (Figure 4a) and the peak current (Figure 4b) of 50 μg L^{-1} Pb^{2+} in pH 4.5 acetate buffer at the flow rate of 1

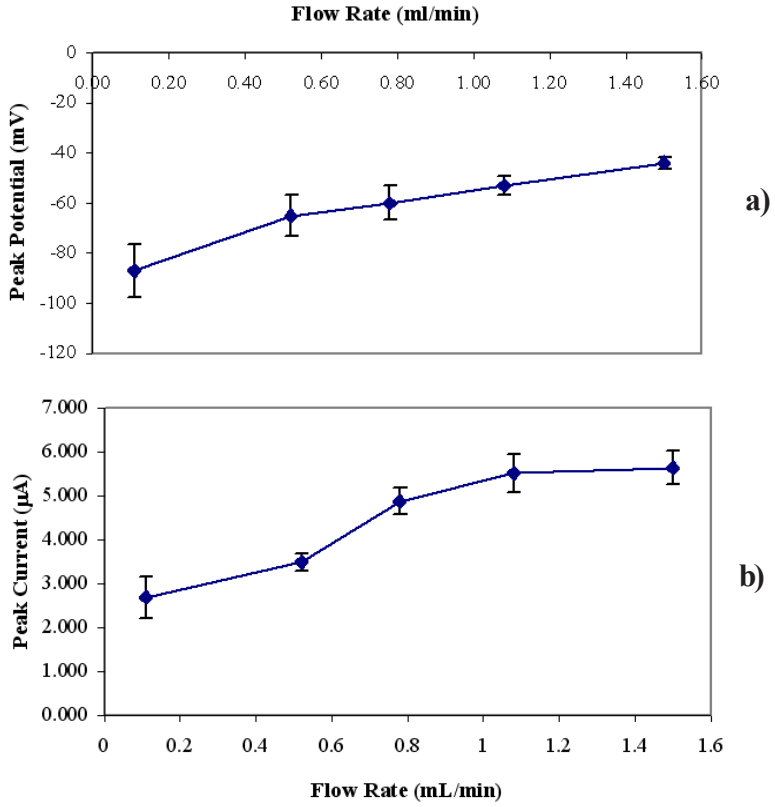

Figure 5. Dependence of the flow rate on (a) the peak potential and (b) on the peak stripping current for 50 µg L^{-1} Pb^{2+} in pH 4.5 acetate buffer at the spacer thickness of 0.125 mm after 60 s electrodeposition, other conditions as in Figure 4. n = 3.

mL min^{-1} and after 60 s electrodeposition at –0.7 V vs Ag/AgCl reference electrode. When the spacer thickness of 0.050 mm was used, the well-defined Pb^{2+} oxidation peaks were observed at approximately –0.09 V. The peak potential of Pb^{2+} was shifted to more positive values after increasing the spacer thickness. However, the well-defined Pb^{2+} oxidation peaks were observed at approximately –0.07 V when the spacer thickness was more than 0.125 mm. As expected the increase in peak current with increasing spacer thickness was observed. However, when the spacer thickness was exceeded 0.125 mm, the resulting peak current decreased and a plateau was reached after 0.250 mm thickness. This is due to the increased diffusion layer in the thin-layer cell and the resulting decrease in reaction time of analytes at the electrode surface. Thus the spacer thickness of 0.125 mm was chosen.

Figure 5 shows the influence of the flow rate on peak potential (Figure 5a) and peak current (Figure 5b) of 50 µg L^{-1} Pb^{2+} in pH 4.5 acetate buffer at the chosen spacer thickness and after 60 s electrodeposition at –0.7 V. The peak potential was shifted to more positive values with increasing flow rate. During the stripping phase, the increase in peak current with increasing flow rate was observed but increased slightly when the flow rate was more than 1.08 mL min^{-1}. Therefore the flow rate of 1.08 mL min^{-1} was chosen.

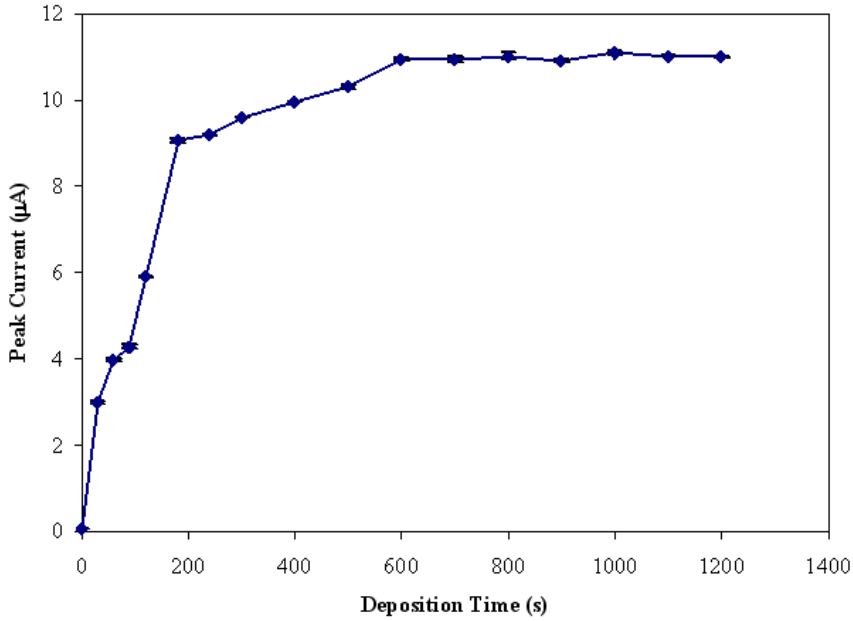

Figure 6. Dependence of the peak current on deposition time for 50 μg L^{-1} Pb^{2+} in pH 4.5 acetate buffer. Square-wave anodic stipping voltammetry for Pb^{2+} at the spacer thickness of 0.125 mm and the flow rate of 1.08 mL min^{-1}, other conditions as in Figure 4. n = 3.

The behaviour of the thin-layer electrochemical flow-through cell at gold disc electrode with increasing deposition time was investigated using a 50 μg L^{-1} Pb^{2+} in pH 4.5 acetate buffer at the chosen spacer thickness and flow rate. The deposition time was varied from 0 to 1200 s. Figure 6 illustrates the dependence of the deposition time on lead response. As expected the peak current increased with increasing deposition time, however a plateau was found to be reached after 600 s deposition. A preconcentration time of 30 s was selected as a good compromise between length of analysis time and sensitivity for routine analysis (total analysis time per sample was only 90 s).

The calibration plots were found to be linear over the concentration range 0-50 mg L^{-1} Pb^{2+}, y = 38.9x, r^2 = 0.992 (n=5) at 30 s deposition and y = 407.6x + 577.1, r^2= 0.996 (n=3) at 600 s deposition. The limit of detection was calculated by making replicated current measurements at –0.1 V for 5 μg L^{-1} Pb^{2+}standard solution; the detection limit based on three times the mean (n=20) of these measurements at 600 s deposition time gave a value of 0.38 μg L^{-1} Pb^{2+}. The coefficient of variation was determined by performing twenty replicate measurements of solution containing 5 μg L^{-1} $Pb^{2+}$and was found to be 2.1 %. The detection limit for a 30 s electrodeposition was also calculated to be 3.5 μg L^{-1}.

3.3 Effect of Other Metal Cations

The effect of other metal cations on lead stripping response was investigated by adding 500 μg L^{-1} of Zn^{2+}, Fe^{2+}, Cu^{2+}, Cd^{2+}, Cr^{6+}, and Hg_2^{2+} to the 50 μg L^{-1} Pb^{2+}standard in pH 4.5 acetate buffer and the reduction in responses are given in Table 1. Like the result when using gold-coated SPCE [19], the

Table 1. Effect of the addition of other metal cations in 50 μg L^{-1} Pb^{2+} in pH 4.5 acetate buffer using the thin-layer cell at gold disk electrode.

Pb(II)	Peak Current (μA)						% Decrease*[25]
	1	2	3	mean	S.D.	%RSD	
alone	3.304	3.350	3.412	3.355	0.04	1.3	0
with Zn(II)	2.214	1.727	2.206	2.049	0.23	11.1	38.9
with Fe(II)	2.495	2.524	2.894	2.638	0.18	6.9	21.4
with Cu(II)	1.582	1.583	1.473	1.546	0.05	3.3	53.9
with Cd(II)	4.424	4.678	4.671	4.591	0.12	2.6	peak overlap
with Cr(VI)	3.384	3.384	3.357	3.375	0.01	0.4	0
with Hg	No Peak of Pb(II) Found						100

* % Decrease at 500 μg L^{-1} = 100 x [{(peak current of pure lead)-(peak current of lead with each cations)}/(peak current of pure lead)]

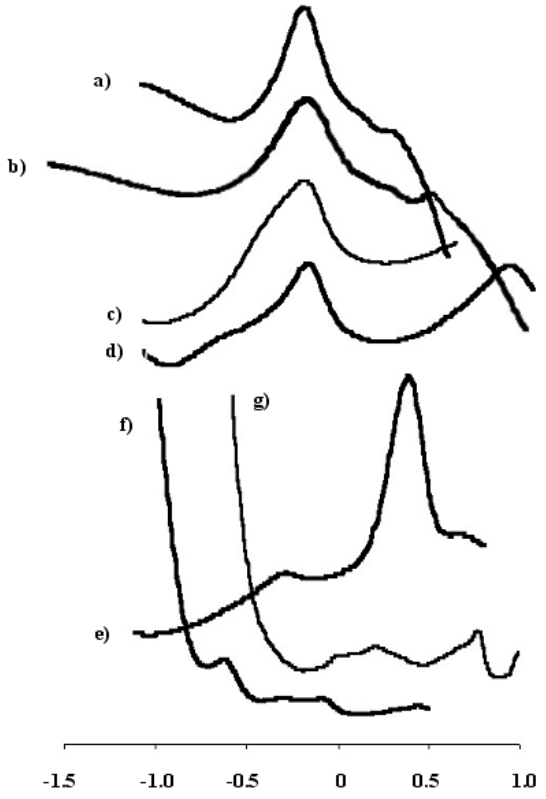

Figure 7. SWASVs obtained on a 50 μg L^{1} Pb^{2+} solution: a) in pH 4.5 acetate buffer only; b) to g) as a) but also containing 500 μg L^{-1} of Cr^{6+}, Cd^{2+}, Fe^{2+}, Cu^{2+}, Zn^{2+}, and Hg_2^{2+}, respectively, other conditions as in Figure 4.

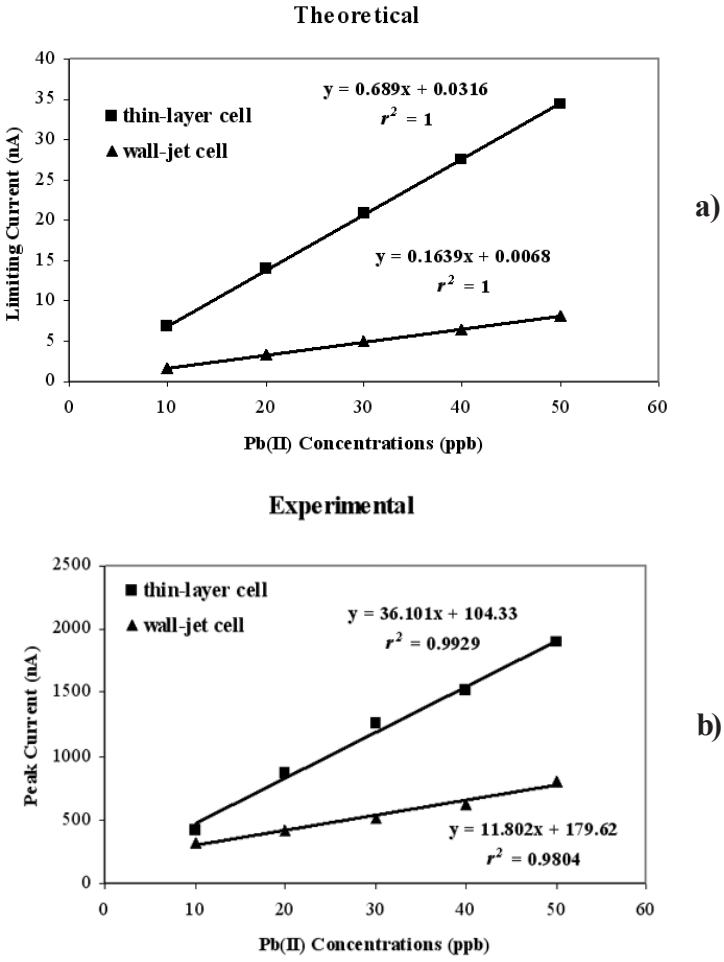

Figure 8. Theoretical (a) and experimental (b) calibration curves for the designed thin-layer and wall-jet cells. The experimental curve was performed at 30 s electrodeposition, other conditions as in Figure 4.

presence of Hg_2^{2+} completely prevented lead measurement by blocking the gold surface with a sorbed layer that was subsequently reduced. Cu^{2+}, Zn^{2+}, and Fe^{2+} reduced the lead response significantly. Cu^{2+} and Zn^{2+} produced a stripping peak at +0.28 and –0.63 V, respectively and also caused a significant decrease in the lead response, owing to the formation of intermetallic compounds. It was found that Cd^{2+} peak overlapped with Pb^{2+} peak while Cr^{6+} did not significantly interfere with the Pb^{2+} determination (Figure 7).

3.4 Comparison of the Electrode Response Using the Thin-layer and Wall-jet Cells for Pb^{2+} Determination

The theory of thin-layer detectors is based on the relationship derived by Matsuda [26] for the limiting current at a flat plate in an enclosed rectangular channel, with fully developed laminar flow parallel to the surface

$$i = 1.47nFC(DA/b)^{2/3}U^{1/3} \quad (1)$$

where the symbols have their usual significance [27]; in our case the active electrode area, A, is 0.10 cm^2 and the spacer thickness, b, is 0.0125 cm.

Table 2. Comparison of the performance of the specially fabricated thin-layer and wall-jet cells incorporating with a gold disc working electrode for Pb^{2+} determination.

Cell design	Effective cell volume (μL)	Edep (V) vs Ag/AgCl	Flow rate (μL min^{-1})	Epa of Pb^{2+} (V)	Surface area (cm^2)	Sensitivity (nA L μg^{-1})	Sensitivity per unit area (A cm g^{-1})	Coefficient of variation (%)	Detection limit (μg L^{-1})
Wall-jet cell	9.29	-0.70	1.08	-0.12	0.07	11.80(30s)	169(30s)	3.0	8.6(30s)
Thin-layer cell	10.0	-0.70	1.08	-0.10	0.10	38.95(30s)	389(30s)	2.1	3.5(30s)

Table 3. Recovery and precision data for Pb^{2+} obtained on drinking and tap water samples.

Samples	Original concentration (μg L^{-1})	Added (μg L^{-1})	Found (μg L^{-1})	% Recovery (%R.S.D., n = 5)
Drinking water 1	ND	30.0	33.9	113 (1.8)
Drinking water 2	ND	30.0	32.5	108 (2.3)
Tap water 1	ND	30.0	32.9	110 (4.8)
Tap water 2	ND	30.0	31.7	106 (3.4)

Similarly, the limiting current at wall-jet electrodes is described by the relationship

$$i = 0.898nFCD^{2/3}n^{-5/12}a^{-1/2}A^{3/8}U^{3/4} \quad (2)$$

in which the diameter of the jet, a, is 0.1 cm, A is 0.07 cm^2, the kinematic viscosity, n, is estimated as 0.01 cm^2 s^{-1} and the average volume flow rate, U, is 0.02 cm^3 s^{-1} [28].

Equation 1 and 2 can be used to calculate the theoretical maximum currents for the thin-layer and wall-jet cells if they are behaving ideally.

The theoretical calibration curves for an amperometric measurement are given in Figure 8(a). Figure 8(b) shows the actual results obtained. It can be seen that the theory predicts a higher sensitivity for thin-layer cell than for wall-jet cell. The experimental results follow the same response pattern as the theoretical prediction although the actual values are quite different because of the square-wave stripping process and the effect of underpotential deposition on the gold surface.

In this application, the sensitivity of the thin layer cell was significantly better (38.95 nA L μg^{-1}) than the wall jet electrode (11.80 nA L μg^{-1}) (Table 2). Both systems provided similar reproducibility so based on the comparison described above, the thin-layer cell with a gold disc electrode was selected for the routine determination of Pb^{2+} in water samples.

3.5 Analytical Application

The proposed specially fabricated thin-layer cell at gold disc electrode was evaluated by carrying out Pb^{2+} determination in drinking and tap water samples before and after spiking with Pb^{2+} at a concentration of 30 μg L^{-1}. The deposition time of 30 s at –0.7 V vs Ag/

AgCl reference electrode was used with the chosen spacer thickness and flow rate. The SWASV parameters were the same as used previously. The concentration of Pb^{2+} was determined using the method of standard addition. Table 3 shows the precision and recovery data obtained on the drinking and tap water samples. These data demonstrate that the proposed method has a good promise for the determination of Pb^{2+} in real samples such as water samples.

4. CONCLUSIONS

Gold electrode microcells in both a wall jet and thin layer configuration can be used for the underpotential anodic stripping voltammetric determination of lead. By incorporating the cells in a flow injection system, a simple, accurate, and reproducible method suitable for routine analysis of Pb^{2+} has been demonstrated. The detection limit depends on the preconcentration time and for the optimum configuration exceeded 0.35 μg L^{-1}. This is a significant improvement on previously reported measurements for lead using mercury-free electrode where detection limits of 16.6 mg L^{-1} are described [18].

ACKNOWLEDGEMENTS

We gratefully acknowledge the Faculty of Science, Naresuan University for funding this research. Some of devices and windows applications were developed in cooperation with Alpha flow research, Chiang Mai University.

REFERENCES

[1] Breen J. and Stroup C.(Ed), *Lead Poisoning,* Lewis Publishers, CRS Press, Boca Raton, Florida, 1995.

[2] Fang Z., *Flow Injection Separation and Preconcentration,* John Wiley, Chichester, 1993.

[3] Ferreira S.L.C., de Brito C.F., Dantas A.F., de Araujo N.M.L. and Costa A.C.S., Nickel determination in saline matrices by ICP-AES after sorption on Amberlite XAD-2 loaded with PAN, *Talanta*, 1999; **48**: 1173-1177.

[4] Ivanova E., Mol W.V. and Adams F., Electrothermal atomic absorption spectrometric determination of cadmium and lead in blood using flow injection on-line sorption preconcentration in a knotted reactor, *Spectrochim. Acta Part B*, 1998; **53 (6-8)**: 1041-1048.

[5] Bravo-Sánchez L.R., de la Riva B.S.V., Costa-Fernández J.M., Pereiro R. and Sanz-Medel A., Determination of lead and mercury in sea water by preconcentration in a flow injection system followed by atomic absorption spectrometry detection, *Talanta* ,2001; **55 (6)**: 1071-1078.

[6] Ma R. and Adams F., Flow injection sorbent extraction with dialkyldithiophosphates as chelating agent for the determination of cadmium, copper and lead by flame atomic absorption spectrometry, *Spectrochim. Acta Part B*, 1996; **51 (14)**: 1917-1923.

[7] Wang J., Hansen E.H. and Gammelgaard B., Flow injection on-line dilution for multi-element determination in human urine with detection by inductively coupled plasma mass spectrometry, *Talanta*, 2001; **55 (1)**: 117-126.

[8] Li J., Lu F., Umemura T. and Tsunoda K., Determination of lead by hydride generation inductively coupled plasma mass spectrometry, *Anal. Chim. Acta*, 2000; **419 (1)**: 65-72.

[9] Castillo E., Cortina J.L., Beltrán J., Prat M.D. and Granados, M., Simultaneous

determination of Cd(II), Cu(II) and Pb(II) in surface waters by solid phase extraction and flow injection analysis with spectrophotometric detection, *Analyst*, 2001; **126 (7)**: 1149-1153.

[10] Luconi M., Silva M. F., Olsina R.A. and Fernandez L., Flow injection spectrophotometric analysis of lead in human saliva for monitoring environmental pollution, *Talanta*, 2001; **54 (1)**: 45-52.

[11] Schneider J.A. and Hornig J.F., Spectrophotometric determination of lead in tap water with 5,10,15,20-tetra (4-N-sulfoethylpyridinium)porphyrin using merging zones flow injection, *Analyst*, 1993; **118 (7)**: 933-936.

[12] Yang X., Hibbert D.B. and Alexander, P.W., Flow injection potentiometry by poly(vinyl chloride)-membrane electrodes with substituted azacrown ionophores for the determination of lead(II) and mercury(II) ions, *Anal. Chim. Acta*, 1998; **372 (3)**: 387-398.

[13] Wang J., *Stripping Analysis: Principles, Instrumentation and Applications,* VCH: Deerfield Beach, Florida, 1985.

[14] Mannino S., Potentiometric stripping analysis of lead and tin with a continuous flow system, *Analyst*, 1984; 109: 905-907.

[15] Matysik F.M. and Werner G., Trace metal determination in tears by anodic stripping voltammetry in a capillary flow injection system, *Analyst*, 1993; **118**: 1523-1526.

[16] Jaenicke S., Sabarathinam R.M., Fleet B. and Gunasingham, H., Determination of lead in blood by hydrodynamic voltammetry in a flow injection system with wall-jet detector, *Talanta*, 1998; **45**: 703-711.

[17] da Silva C.L. and Masini J.C., Determination of Cu, Pb, Cd, and Zn in River Sediment Extracts by Sequential Injection Anodic Stripping Voltammetry with Thin Mercury Film Electrode, *Fresenius' J. Anal. Chem.*, 2000; **367 (3)**: 284-290.

[18] van Staden J.F. and Matoetoe M.C., Simultaneous determination of copper, lead, cadmium and zinc using differential pulse anodic stripping voltammetry in a flow system, *Anal. Chim. Acta*, 2000; **411**: 201-207.

[19] Masawat P., Liawruangrath S. and Slater J.M., Flow injection measurement of lead using mercury-free disposable gold-sputtered screen-printed carbon electrodes (SPCE), *Sens. Actuators B*, 2003; **91**: 52-59.

[20] Laxen D.P.H. and Harrison R.M., Cleaning methods for polythene containers prior to the determination of trace metals in freshwater sample, *Anal. Chem.*, 1981; **53**: 345-350.

[21] Masawat P., Liawruangrath S., Vaneesorn Y. and Liawruangrath B., Design and fabrication of a low-cost flow-through cell for the determination of acetaminophen in pharmaceutical formulations by flow injection cyclic voltammetry, *Talanta*, 2002; **58**: 1221-1234.

[22] Kolb D.M., Prazasnyske M. and Gerischer H., Underpotential deposition of metals and work function differences, *J. Electroanal. Chem.*, 1974; **54**, 25-38.

[23] Kolb D.M. (Ed), Gerischer H. and Tobias C.W., *Advances in electrochemistry and electrochemical engineering,* John Wiley Interscience, New York, 1978; 11, 125.

[24] Aramata A. (ED), Bockris J.O'M., White R.E. and Conway B.E., *Modern aspects of electrochemistry,* Plenum, New York, 1997; 31, 181.

[25] van Staden J.F. and Matoetoe M., Determination of copper by anodic stripping voltammetry on a glassy carbon electrode using a continuous flow system, *Fresenius' J. Anal. Chem.*, 1997; **357**: 624-628.

[26] Matsuda H., Zur theorie der stationären strom-spannunos-kurven von redox-elektrodenreaktionen in hydrodynamischer voltammetrie: II. laminare rohr- und kanalstkömungen, *J. Electroanal. Chem.*, 1967; **15**: 325-336.

[27] Elbicki J.M., Morgan D.M. and Weber S.G., Theoretical and practical implications on the optimization of amperometric detectors, *Anal. Chem.*, 1984; **56**: 978-985.

[28] Matsuda H., Zur theorie der stationären strom-spannungs-kurven von redox-elektrodenreaktionen in hydrodynamischer voltammetrie: I. laminare staupunktströmltngen, *J. Electroanal. Chem.*, 1967; **15**: 109-127.